

On the nature of radio filaments near the Galactic Center

Maxim V. Barkov^{1,2,3*}, and Maxim Lyutikov¹

¹ *Department of Physics and Astronomy, Purdue University, West Lafayette, IN 47907-2036, USA*

² *Astrophysical Big Bang Laboratory, RIKEN, 351-0198 Saitama, Japan*

³ *Space Research Institute of the Russian Academy of Sciences (IKI), 84/32 Profsoyuznaya Str, Moscow, Russia, 117997*

Received/Accepted

ABSTRACT

We suggest that narrow, long radio filaments near the Galactic Center arise as kinetic jets - streams of high energy particles escaping from ram-pressure confined pulsar wind nebulae (PWNe). Reconnection between the PWN and interstellar magnetic field allows pulsar wind particles to escape, creating long narrow features. They are the low frequency analogues of kinetic jets seen around some fast-moving pulsars, such as The Guitar and The Lighthouse PWNe. The radio filaments trace a population of pulsars also responsible for the Fermi GeV excess produced by the Inverse Compton scattering by the pulsar wind particles. The magnetic flux tubes are stretched radially by the large scale Galactic winds. In addition to PWNe accelerated particles can be injected at supernovae remnants. The model predicts variations of the structure of the largest filaments on scales of \sim dozens of years - smaller variations can occur on shorter time scales. We also encourage targeted observations of the brightest sections of the filaments and of the related unresolved point sources in search of the powering PWNe and pulsars.

Key words: acceleration of particles – stars: neutron — ISM: magnetic fields – Galaxy: centre

1 INTRODUCTION

The central part of the Galaxy shows numerous non-thermal filaments (NTFs) (Yusef-Zadeh et al. 1984; Yusef-Zadeh & Morris 1987; Morris & Serabyn 1996; MeerKAT Collaboration 2018), the largest been the Snake, G359.1-00.2, (Gray et al. 1995).

Key observational facts of NTFs are:

- Filaments are few parsecs to few tens of parsecs long, with mostly linear morphology
- Many NTFs show a clear bright central part, not associated with any resolved source; sometimes NTFs have associated compact sources
 - Some filaments seem to be connected to a SNR
 - Most of the NTFs are perpendicular to the Galactic plane to within 20 degrees (Morris & Yusef-Zadeh 1985; Anantharamaiah et al. 1991)
 - NTFs have constant flat spectral index $F_\nu \propto \nu^0$ (Yusef-Zadeh et al. 1984)
 - Polarization indicates magnetic field along the filaments (Gray et al. 1995; Lang et al. 1999).
 - a turnover of the hard synchrotron spectrum at \sim 10 GHz is observed (Boldyrev & Yusef-Zadeh 2006).

- The brightest NTFs reach a total power of the order of 10^{33} erg s⁻¹

The most natural explanation for the radio filaments is that of a magnetic flux tube populated by highly relativistic particles (Yusef-Zadeh et al. 1984; Yusef-Zadeh & Morris 1987; Morris & Serabyn 1996). Shore & LaRosa (1999); Rosner & Bodo (1996); Boldyrev & Yusef-Zadeh (2006) developed models of NTF as separate hydrodynamic entities. Alternatively, and we favor this interpretation, the observed filaments are the magnetic flux tubes that happen to be illuminated by the local injection of relativistic particles (Morris & Serabyn 1996). But what is the source of these particles?

In the present paper we advance a model of Galactic Center’s NTFs as low frequency analogues of extended features seen around some ram pressure-confined PWN, such as the Guitar (Wong et al. 2003; Hui & Becker 2007; Johnson & Wang 2010) and the Lighthouse (Pavan et al. 2016). Using 3D relativistic MHD simulations Barkov et al. (2019a,b) showed that these features can’t have hydrodynamical origin and have to be kinetically streaming pulsar wind particles that escaped into the interstellar medium (ISM) due to reconnection between the PWN and ISM magnetic fields (see also Bandiera (2008a)).

In our model, see Fig. 2, the magnetic field is accumulated in the gaseous disk (Sofue et al. 1986; Molinari et al.

* Correspondence author: mbarkov@purdue.edu (MVB)

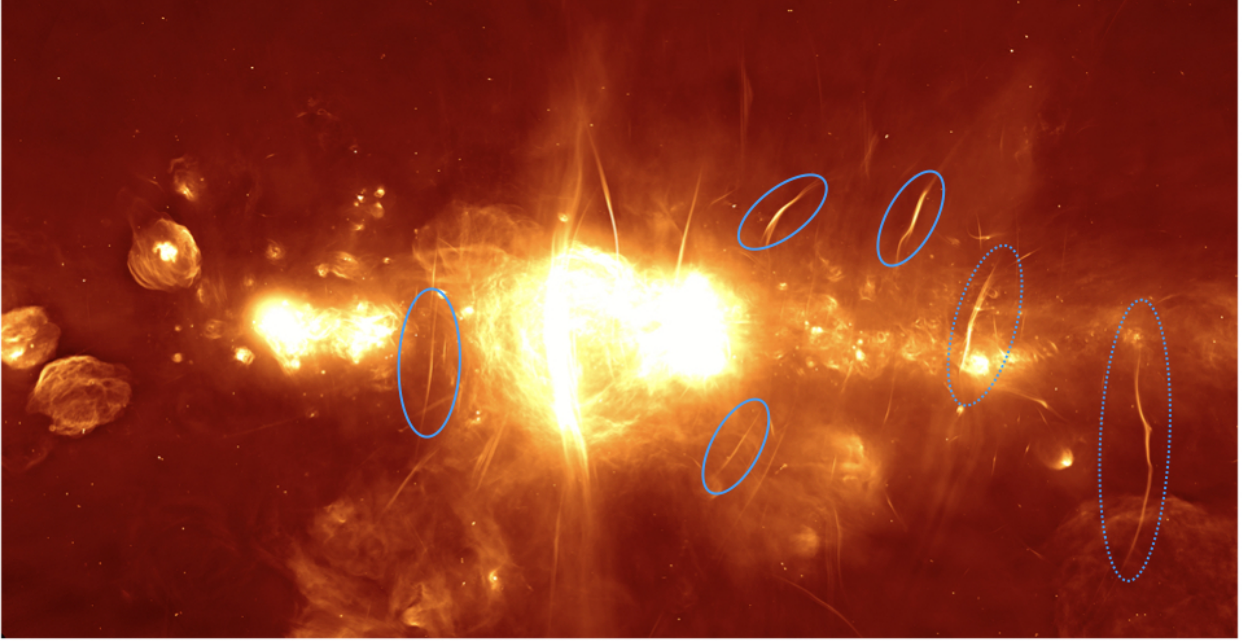


Figure 1. MeerKAT image of the Galactic Center (MeerKAT Collaboration 2018). Highlighted are “orphan” filaments that seem not be connected to any resolved source (solid lines), and filaments that seem to be connected to a SNR (dashed lines).

2011; Barkov & Bosch-Ramon 2014), while the disk winds stretches the field lines open in vertical direction (Ponti et al. 2019). The gas in outflow is hot with characteristic pressure 0.2 eV cm^{-3} , which corresponds to magnetic field strength about 10^{-4} G .

A collection of millisecond pulsars (MPSs) (Bartels et al. 2016) are orbiting the central regions with virial velocities of $\sim 300 \text{ km s}^{-1}$. Interaction of the MPSs with the surrounding plasma creates bow shock PWNe, with sizes too small to be resolved, a fraction of an arcsecond, Eq. (1).

As the pulsars move through ISM, the external magnetic field is draped around PWN creating a narrow layer of near-equipartition magnetic field at the contact discontinuity (Spreiter et al. 1966; Lyutikov 2006; Dursi & Pfrommer 2008). As a result, the contact discontinuity becomes a rotational discontinuity with magnetic fields of similar strength on both sides. Rotational discontinuities are prone to reconnection (see, e.g., Komissarov et al. 2007; Barkov & Komissarov 2016, and references therein). The efficiency of reconnection at a given point on the contact/rotational discontinuity will depend on the relative orientation of the PWN and ISM magnetic fields- reconnection occurs when the internal and external fields are approximately counter-aligned.

As a result, an effective “hole” appears in the PWN through which particles accelerated at the termination shock can escape into the ISM (Barkov et al. 2019b).

2 MAGNETIC FILAMENTS CONNECTED TO RAM PRESSURE CONFINED PWNE

2.1 Length and brightness estimates

Consider a pulsar with spindown power \dot{E} moving with velocity v_p through a medium of particle density n (see e.g. Kargaltsev et al. 2017, for review). The stand-off distance is

$$r_s = \left(\frac{\dot{E}}{4\pi n m_p c v_p^2} \right)^{1/2} = 1.3 \times 10^{-2} E_{35}^{1/2} n_0^{-1/2} v_{p,7}^{-1} \text{ pc}, \quad (1)$$

here m_p is proton mass, c is speed of light. At the distance of 8.2 kpc this corresponds to ~ 0.1 arcsec. In this paper we use the following notation $A_n = A/10^n$ in cgs units.

A typical connection time to a given field lines is time to travel the stand-off distance

$$t_s = \frac{r_s}{v_p} = 1.3 \times 10^2 E_{35}^{1/2} n_0^{-1/2} v_{p,7}^{-2} \text{ yrs} \quad (2)$$

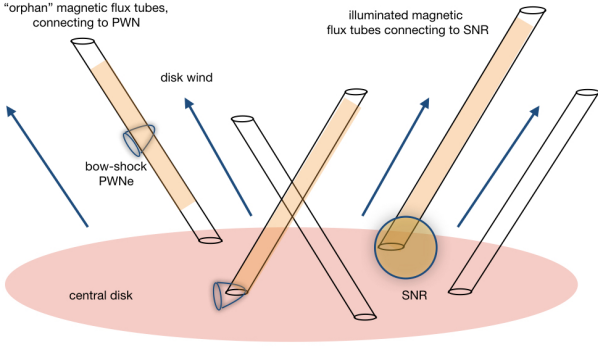


Figure 2. Cartoon of the model. The central disk produces a wind that stretches magnetic field lines. Pulsars orbiting the central bulge produce PWN. Reconnection between the internal PWN magnetic fields and external field allows the relativistic particles to escape creating long non-thermal filaments. Similarly, supernova remnants can also populate the magnetic field lines and produce radio filaments.

Thus a slow pulsar with high \dot{E} pulsar is expected to remain connected to a given flux tube for a long time.

The pulsar produces a wind with typical Lorentz factor $\gamma_w \sim 10^3 - 10^6$ and magnetization σ_w (Kennel & Coroniti 1984). Termination shocks in the nebula accelerate particles to a power law distribution with typical minimal Lorentz factor γ_w . As the particles escape from the PWN and enter the ISM they produce synchrotron emission in the ISM magnetic field. The peak of synchrotron emission at νF_ν have place at 1.33 times higher relative to F_ν , and peak have place at $0.29 \nu_{\text{critical}}$, here

$$\nu_{\text{critical}} = \frac{3}{4\pi} \frac{eB}{m_e c} \gamma_e^2, \quad (3)$$

here e , m_e and γ_e are electron charge, mass and Lorentz factor respectively. Observable frequency is

$$\nu_{\text{rad}} = 0.1 \frac{eB}{m_e c} \gamma_e^2. \quad (4)$$

During the connection time t_s a pulsar produces a number of e^\pm pairs

$$N_\pm = t_s \dot{n}_e \\ \dot{n}_e = \frac{\dot{E}}{\gamma_w \sigma_w m_e c^2} \quad (5)$$

If a fraction η escapes, then the radio luminosity can be estimated as

$$L_{\text{rad}} = N_\pm \frac{2e^4}{3m_e^2 c^3} \gamma_e^2 B^2 \quad (6)$$

and expressing γ_e from Eq. (4), N_\pm from (5), and assuming $\gamma_e = \gamma_w$ we finally get

$$L_{\text{rad}} = 0.6 \frac{\eta e^{7/2} B^{3/2} \nu_{\text{rad}}^{1/2} \dot{E}^{3/2}}{m_p^{1/2} m_e^{5/2} n^{1/2} \sigma_w v_p^2 n^{1/2}} = \\ = 6 \times 10^{31} \frac{\eta \dot{E}_{35}^{3/2} B_{-4}^{3/2} \nu_{10\text{GHz}}^{1/2}}{\sigma_w v_{p,7}^2 n_0^{1/2}} \text{ erg/s} \quad (7)$$

This estimate matches, given a number of the unknown parameters, the maximal radio luminosity of the NTFs.

The corresponding cooling time scale is much longer than the connection time (2):

$$\tau_c \approx \frac{N_\pm m_e c^2 \gamma_e}{L_{\text{rad}}} \approx 2 \times 10^5 B_{-4}^{-3/2} \nu_{10\text{GHz}}^{-1/2} \text{ yrs} \quad (8)$$

This explains the homogeneous spectral index along the filaments.

As an example, consider the largest filament G359.1-00.2 (the Snake, Gray et al. 1995). It has length of $300'' = 12$ pc (at the distance of 8.2 kpc), width $10'' = 0.4$ pc, maximal surface brightness 10^{-4} Jy arcsec $^{-2}$. The total luminosity at 5GHz evaluates to 10^{32} erg s $^{-1}$.

The length and the luminosity are consistent with our estimates (2) and (6). The apparent thickness of the filament may increase both to field meandering and to kinetic scattering of the escaped particles by the MHD turbulence in the ISM.

2.2 Possible kinks in the NTFs

The Snake shows an interesting feature resembling a kink. This can be produced by the charged flow of the PWN wind driving the current along the filament. The pulsar produces a charge-separated flow that carries a total current $I \sim \sqrt{\dot{E}c}$. If the connection of the external field line is such that a fraction of that current escapes with the kinetic flow of the particles through a flux tube of size ηr_s , then the resulting toroidal magnetic field is

$$B_\phi \approx \eta_c \frac{\dot{E}^{1/2}}{2\pi \sqrt{c} \eta r_s} \quad (9)$$

A kink will occur if toroidal field (9) is larger than the external field. This requires

$$\frac{\eta_c}{\eta} \geq \frac{B}{\sqrt{m_p n v_p}} \approx 10 \quad (10)$$

Thus, under certain conditions the escaping kinetic jet may carry enough current to become kink unstable. (Since the pulsar wind is a charge-separated flow, the escaping current is carried by charge density (not the relative motion of charges). Electrostatic effects may further complicated the global dynamics.

2.3 Fermi and VHE excess towards the GC

The model is possibly related to the Fermi and VEH gamma-ray excess towards the GC. The GC gamma-ray signal peaks at ~ 100 MeV with total power $\sim \text{few} \times 10^{36}$ erg s $^{-1}$ (see Fig. 8 in van Eldik 2015). Though the VHE part of the excess is clearly of hadronic origin, the GeV-TeV range may have a different origin. Population of milliseconds pulsars seems to be the best explanation (Bartels et al. 2016). Thousands of MSPs are needed.

We suggest that IC scattering by the pulsars' wind particles can contribute to the 100 MeV-100 GeV photon flux. In the present model, the central pulsars produce a relativistic wind that eventually mixes with the ISM. The pulsar wind particles up-scatter via Inverse Compton process the

soft photons. For a soft photon of energy ϵ_s the expected IC energy is

$$\epsilon_{IC} \sim \gamma_e^2 \epsilon_s = 10^8 \gamma_{e,4}^2 \epsilon_{s,0} \text{eV}, \quad (11)$$

here ϵ_s energy of soft photons is measured in eV. This matches the observed spectral peak of the GC gamma-ray excess.

The IC luminosity can be estimated using the following assumptions: (i) photon energy density is a fraction of the magnetic field energy density $u_{ph} = \eta_E B^2 / (8\pi)$; (ii) cooling is determined by synchrotron losses. The IC luminosity is then the number of pulsars N_p , times the number of particles a pulsar injects during cooling time scale, $\dot{n}\tau_c$ (all particles contribute to the IC signal, not only those that escapes), times the IC power of each particle. This gives

$$L_{IC} \approx \frac{\eta_E}{\sigma_w} N_p \dot{E} \quad (12)$$

Thus, few hundred to a thousand pulsars with spindown power of $\dot{E} \sim 10^{33} - 10^{34} \text{ erg s}^{-1}$ can produce the required power of the GeV signal from the GC.

2.4 Predictions

The model has a number of clear predictions

- Most importantly, the NTFs should vary on fairly short time scales, dozens of years, Eq. (2). Smaller variations can feasibly be detected on shorter time scales (compare with variations seen in the NTF associated with the Guitar Nebula, Chatterjee & Cordes 2004).
- The pulsar powering the filaments is most likely located near the brightest section of the filament.
- Similarly, many filaments show compact sources - these could be the powering bow-shock PWNe. These PWNe harbor pulsars.
- Since higher \dot{E} pulsars remain connected to a given flux tube for longer time, Eq. (2), the searchers for pulsars should prefer bright and *long* wisps.

Since the filaments are located towards a dense CG region, scattering of time-variable radio sources is important. Going to higher frequencies reduces the effects of scattering, but (i) pulsars are weaker at higher frequencies; (ii) radio telescopes beams are narrower. Perhaps the best frequency range is 2 – 5 GHz. At these frequencies the GBT beam is about arcminute. Filaments are few arcmin long and less than arcmin thick - this matches the resolution of the GBT. We encourage observations of central parts of the filaments and associated point sources in search of pulsars. (We thank Scott Ransom for pointing out these details.)

3 DISCUSSION

We discuss the origin of Galactic Center radio filaments as kinetic jet powered by the particle accelerated in bow shock PWNe. In our interrelation the filaments are not hydrodynamically separate entities - there are just illuminated by a present of accelerated particles that propagate *kinetically*. They are the low frequency analogues of kinetic jets seen around some fast-moving pulsars, such as the Guitar and the

Lighthouse Kargaltsev & Pavlov (2008); Bandiera (2008b); Barkov et al. (2019b).

Let us next discuss how the model explains the key observational facts

- the length of filaments reflects the duration of connection of a given field line to a PWN, Eq. (2); linearly morphology reflects the field lines stretched radially by the galactic wind
- compact sources associated with NTFs are the unresolved PWNe harboring pulsars
- orientation of the NTFs is determined by the Galactic wind that stretches the magnetic field lines; this also determines polarization
- Sometimes NTFs split into multiple filaments running parallel to each other Lang et al. (1999) - this reflects the non-stationary process of magnetic reconnection that “opens” and “closes” the pulsar magnetosphere.

An important advantage of the present model over previous suggestions (*e.g.* tails of bow shock PWN/analogues of cometary tails (Shore & LaRosa 1999), or other hydrodynamic flows (Rosner & Bodo 1996)) is that the non-thermal particles and magnetic field within the NTFs should not be in a pressure balance with the surrounding mediums (such requirement puts high demands on the correspond magnetic field and particle energy density). The emission is produced by a population of kinetically - as opposed to hydrodynamically-propagating particles whose pressure and energy density are small if compared with the thermal plasma energy density.

One can imagine two possible types of structure of the magnetic field: a nearly completely volume-filling magnetic field, whereby only selected flux tubes are lit due to reconnection with the PWN. Alternatively, the magnetic field is highly inhomogenous and pulsar lit up the high magnetic field regions. The most feasible scenario can be superposition of two mentioned above.

Finally, some NTFs seem to connect to individual SNRs or to large scale bubbles formed by merged SNRs or Particle source in the galactic center. SNRs are well known source of accelerated non-thermal leptons (Uchiyama & Aharonian 2008). Non-thermal particles that can escape along magnetic fields and can produce similar extended features. If SNR is an origin, one then expects a kinetic jet on both sides. One possibility is that kinetic jets end in SNRs: locally generated turbulence impedes propagation of particles, terminating the kinetic jet. The drop of magnetic field intensity on the scale SNR also can explain strong asymmetry of NTFs. We leave these hypotheses as an open question for further studies.

ACKNOWLEDGMENTS

This work had been supported by DoE grant DE-SC0016369 and NASA grant 80NSSC17K0757.

We would like to thank Matthew Bailes, Bill Cotton, Maura McLaughlin, Scott Ransom, Ingrid Stairs, Farhad Zadeh for discussions.

REFERENCES

- Anantharamaiah K. R., Pedlar A., Ekers R. D., Goss W. M., 1991, *MNRAS*, **249**, 262
- Bandiera R., 2008a, *A&A*, **490**, L3
- Bandiera R., 2008b, *A&A*, **490**, L3
- Barkov M. V., Bosch-Ramon V., 2014, *A&A*, **565**, A65
- Barkov M. V., Komissarov S. S., 2016, *MNRAS*, **458**, 1939
- Barkov M. V., Lyutikov M., Khangulyan D., 2019a, *MNRAS*, **484**, 4760
- Barkov M. V., Lyutikov M., Klingler N., Bordas P., 2019b, *MNRAS*, **485**, 2041
- Bartels R., Krishnamurthy S., Weniger C., 2016, *Physical Review Letters*, **116**, 051102
- Boldyrev S., Yusef-Zadeh F., 2006, *ApJ*, **637**, L101
- Chatterjee S., Cordes J. M., 2004, *ApJ*, **600**, L51
- Dursi L. J., Pfrommer C., 2008, *ApJ*, **677**, 993
- Gray A. D., Nicholls J., Ekers R. D., Cram L. E., 1995, *ApJ*, **448**, 164
- Hui C. Y., Becker W., 2007, *A&A*, **467**, 1209
- Johnson S. P., Wang Q. D., 2010, *MNRAS*, **408**, 1216
- Kargaltsev O., Pavlov G. G., 2008, in Bassa C., Wang Z., Cumming A., Kaspi V. M., eds, American Institute of Physics Conference Series Vol. 983, 40 Years of Pulsars: Millisecond Pulsars, Magnetars and More. pp 171–185 ([arXiv:0801.2602](https://arxiv.org/abs/0801.2602)), [doi:10.1063/1.2900138](https://doi.org/10.1063/1.2900138)
- Kargaltsev O., Pavlov G. G., Klingler N., Rangelov B., 2017, *Journal of Plasma Physics*, **83**, 635830501
- Kennel C. F., Coroniti F. V., 1984, *ApJ*, **283**, 694
- Komissarov S. S., Barkov M., Lyutikov M., 2007, *MNRAS*, **374**, 415
- Lang C. C., Morris M., Echevarria L., 1999, *ApJ*, **526**, 727
- Lyutikov M., 2006, *MNRAS*, **373**, 73
- MeerKAT Collaboration 2018, Monthly Notes of the Astronomical Society of South Africa, **77**
- Molinari S., et al., 2011, *ApJ*, **735**, L33
- Morris M., Serabyn E., 1996, *ARA&A*, **34**, 645
- Morris M., Yusef-Zadeh F., 1985, *AJ*, **90**, 2511
- Pavan L., et al., 2016, *A&A*, **591**, A91
- Ponti G., et al., 2019, *Nature*, **567**, 347
- Rosner R., Bodo G., 1996, *ApJ*, **470**, L49
- Shore S. N., LaRosa T. N., 1999, *ApJ*, **521**, 587
- Sofue Y., Fujimoto M., Wielebinski R., 1986, *ARA&A*, **24**, 459
- Spreiter J. R., Summers A. L., Alksne A. Y., 1966, *Planet. Space Sci.*, **14**, 223
- Uchiyama Y., Aharonian F. A., 2008, *ApJ*, **677**, L105
- Wong D. S., Cordes J. M., Chatterjee S., Zweibel E. G., Finley J. P., Romani R. W., Ulmer M. P., 2003, in Li X. D., Trimble V., Wang Z. R., eds, IAU Symposium Vol. 214, High Energy Processes and Phenomena in Astrophysics. p. 135
- Yusef-Zadeh F., Morris M., 1987, *ApJ*, **322**, 721
- Yusef-Zadeh F., Morris M., Chance D., 1984, *Nature*, **310**, 557
- van Eldik C., 2015, *Astroparticle Physics*, **71**, 45